Acta Neuropathol (1989) 78:605–614

Acta Neuropathologica

Morphological consequences of early reperfusion following thrombotic or mechanical occlusion of the rat middle cerebral artery*

W. D. Dietrich[1,2,3], H. Nakayama[3], B. D. Watson[1,3], and H. Kanemitsu[3]

Departments of [1] Neurology (D 4–5), [2] Anatomy and Cell Biology[3], Cerebral Vascular Disease Research Center, University of Miami School of Medicine, P. O. Box 016960, Miami, FL 33101, USA

Summary. The early morphological consequences of recirculation following middle cerebral artery (MCA) occlusion were studied in two rat models. The proximal MCA was occluded for 1 h by either a surgical clip or platelet thrombus; subsequently, 1 h of recirculation was facilitated. Following clip occlusion and recirculation, mild astrocytic swelling, especially around blood vessels, was detected in reperfused cortical and striatal areas. Neuronal changes included slight chromatin clumping and dilation of the rough endoplasmic reticulum. In contrast, severe structural abnormalities were detected following recanalization of the thrombosed MCA segment. Marked astrocytic swelling of cell bodies and perivascular processes with neuropil vacuolation were commonly seen. A heterogeneous pattern of neuronal alterations, including a high frequency of dense shrunken neurons surrounded by swollen astrocytic processes was documented in cortical and striatal regions. Severe neuronal changes were documented in brain regions exhibiting a well-perfused microcirculation. Vascular endothelial cells contained large numbers of pinocytotic vesicles associated with luminal and abluminal surfaces. Pronounced and rapid morphological changes evolve with reperfusion when thrombotic and ischemic events occur simultaneously. The basis for these rapid parenchymal changes following vascular thrombosis may involve acute alterations in cerebral microvascular permeability which exacerbate ischemic consequences.

Key words: Blood-brain barrier – Ischemia – Middle cerebral artery occlusion – Thrombosis

* Supported by USPHS grants NS-05820 and NS-23244, National Parkinson Foundation Grant YR 660068, and by the American Heart Association Grant-in-Aid 87-1012, with funds contributed by the Florida Affiliate. W. Dalton Dietrich is an Established Investigator of the American Heart Association.

Offprint requests to: W. D. Dietrich (address see above)

Experimental studies have demonstrated that in the initial stages of cerebral ischemia, the blood-brain barrier (BBB) to macromolecules is relatively intact [17, 31, 33]. Increased cerebrovascular permeability, leading to serum protein extravasation, vasogenic edema and severe brain swelling, may require hours or days to develop following mechanical occlusion of a large cerebral vessel [14, 21, 22, 30, 34]. Autoradiographic data obtained in normotensive rats have also failed to document acute BBB alterations following permanent middle cerebral artery (MCA) occlusion. Using [^{14}C]aminoisobutyric acid as a tracer to study alterations in cerebral microvascular permeability, Tyson et al. [40] failed to demonstrate an increase in capillary permeability at 4 h after MCA occlusion. In contrast, experimentally induced vascular thrombosis of large cerebral vessels is associated with acute BBB changes [8, 9]. In one study, photochemically induced MCA thrombosis led to widespread BBB alterations at 15 min following the vascular insult [8]. These results indicate that the early consequences of a pure ischemic insult on the cerebral microvasculature and those observed following vascular thrombosis may differ.

In the context of postischemic reperfusion, acute BBB alterations might be expected to worsen the detrimental effects of cerebral ischemia. For example, Ting et al. [39] have presented evidence suggesting that BBB opening to proteins during the acute stages of recirculation following MCA occlusion in cats is associated with severe post-ischemic edema and increased ischemic brain injury. Although various studies have investigated the consequences of reperfusion following cerebral ischemia [10, 18, 19, 24, 25, 35, 36, 39], the early morphological consequences of reperfusion following thrombotic occlusion have not been investigated.

We have recently shown that the proximal portion of the MCA of rats can be occluded by a nonfibrin-stabilized platelet thrombus induced in situ by a

photochemical technique [8, 28, 42]. In this model, recirculation can be induced by the topical application of the calcium-entry blocker nimodipine, resulting in vasodilation of the occluded MCA segment with ensuing fragmentation and dispersion of the thrombotic material [28]. The objective of the present study was to compare the early morphological consequences of reperfusion following thrombotic or mechanical occlusion of the MCA. In each model, light and electron microscopic techniques were used to document neuronal and vascular changes associated with these different methods of MCA occlusion.

Methods

Animal preparation

Normally fed male Sprague-Dawley rats, weighing 250–320 g, were used in these studies. Anesthesia was induced with 4% halothane, maintained with 1.5% halothane, 70% nitrous oxide and a balance of oxygen delivered through a closely fitting face mask. Polyethylene catheters were inserted retrogradely into the right external carotid artery and right femoral artery and vein. Rectal temperature was maintained at 37° C by means of a heating pad. Rats were mounted on a stereotaxic frame and the right MCA was exposed by a modified subtemporal approach [28, 37].

MCA thrombosis and recanalization

Photochemically induced MCA occlusion ($n = 4$) was carried out by a low-power He-Ne laser operating at 0.8 mW at a wavelength of 543.5 nm (PMS Electro-Optics, Boulder, Colo., USA). The ring-shaped (TEM_{01}* mode) beam was focused transversely onto the exposed MCA by two crossed cylindrical lenses of 1- and 2-inch focal length. The resulting focussed spot was line-shaped and spanned the diameter of the MCA perpendicular to its axis. The linear beam was first focused transversely on the MCA segment just distal to the rhinal branch. The intensity of the laser irradiation at the focal site was 10 W/cm^2. Rose bengal was injected intravenously (30 mg/ml in saline, 0.67 ml/kg body weight). Within 10 min, the MCA was completely occluded by a white thrombus. The laser beam was then moved to the horizontal portion of the MCA, distal to the olfactory tract and proximal to the rhinal branch. Following a second injection of rose bengal, another thrombus was then induced at this site. By the end of the second irradiation, a thrombus of approximately 1.2 mm in length was present in the MCA, centered at the olfactory tract [28].

At 1 hour (h) after the induction of MCA thrombosis, the dura was incised along the MCA, and 150 µl of 20 µM nimodipine was applied to the entire thrombosed MCA segment. Immediately thereafter, blood was observed to infiltrate at both ends of the thrombus, with complete recanalization being achieved in 2 min. Control rats ($n = 2$) underwent all surgical procedures and were injected with rose bengal but not irradiated. These rats were perfusion-fixed 2 h later.

Mechanical occlusion of MCA with recirculation

Immediately distal to the olfactory tract, the dura was incised and a specially designed microvascular clip was placed on the MCA of four rats [2]. Complete MCA occlusion was confirmed by inspection of the vessel during the injection of a 100 µl saline bolus through the retrograde external carotid catheter. After 1 h, the clip was removed and reperfusion of the previously occluded vessel visually confirmed. Control rats ($n = 3$) underwent all surgical procedures including MCA localization and incision of the overlying dura. Control rats were perfusion-fixed 2 h later.

Three additional rats were used to determine whether the topical application of nimodipine to the occluded MCA segment influenced the histopathological response to mechanical occlusion. For these studies the MCA was occluded for 1 h with a surgical clip as previously described. Immediately following clip removal, 150 µl of 20 µM nimodipine was topically applied to the previously occluded MCA segment. Vasodilation of the exposed MCA segment and other vessels running in the operated field was observed. This procedure, therefore, mimicked the steps carried out to recanalize the thrombosed MCA.

Ultrastructural procedures

One hour following recanalization, rats were perfusion fixed with a mixture of 2% paraformaldehyde and 2.5% glutaraldehyde in a 0.1 M sodium phosphate buffer. Perfusion pressure was monitored throughout the procedure and maintained at 110 mm Hg. Following perfusion, the brain was removed from the cranial vault and placed in fresh chilled fixative (4° C) for 2 h. The brain was then returned to chilled 0.1 M sodium phosphate buffer at 4° C for 2 h. With the aid of a dissecting microscope, the previously thrombosed or clipped segment of the MCA was dissected free from the surface of the brain and placed in buffer. The MCA was then cut longitudinally with a scalpel blade to expose the luminal surface. Brains were sectioned into coronal blocks containing the occluded MCA territories, mounted on an Oxford Vibratome and completely sectioned at 150 µm in the coronal plane.

Adjacent sections were processed for routine scanning (SEM) or transmission electron microscopy (TEM) as previously described [6]. In either case, tissue was next post-fixed in sodium phosphate-buffered 1% osmium tetroxide for 1 h. Brain sections chosen for SEM along with the MCA specimens were dehydrated in graded ethanols and placed in freon. Tissue was then critical-point dried, coated with gold and examined and photographed with a JEOL 35C scanning electron microscope. For TEM, areas of interest including frontoparietal somatosensory cortex and dorsolateral striatum (ipsilateral to occlusion) were dissected from the Vibratome sections, immersed in buffer and processed. Thick plastic sections (1 µm) were stained with toluidine blue and examined and photographed with a light microscope. To determine the relative extent of neuronal changes in these specimens, numbers of normal-appearing neurons, neurons with microvacuolated cytoplasm and clumped nuclear chromatin, and dark shrunken neurons were determined in cortical and striatal brain regions. For each rat, four thick sections of somatosensory cortex and four sections of dorsolateral striatum were analyzed. In each section, neuronal counts were made on four microscopic fields ($\times 400$). Thin sections were next cut with a diamond knife, stained with uranyl acetate and lead citrate and examined and photographed in a Zeiss EM-10C transmission electron microscope.

Results

Physiological and control findings

Physiological findings from control and experimental rats prior to MCA occlusion are presented in Table 1.

Table 1. Physiological variables immediately prior to occlusion of the middle cerebral artery (MCA)

	Control ($n = 5$)	Thrombosis ($n = 4$)	Clip ($n = 4$)	Clip + Nimodipine ($n = 3$)
PCO_2 (mm Hg)	49.6 ± 3.7	50.5 ± 1.7	50.1 ± 1.3	55.5 ± 2.5
PO_2 (mm Hg)	132.7 ± 10	138.9 ± 13	143.8 ± 18	137.5 ± 8
pH (units)	7.25 ± 0.01	7.38 ± 0.02	7.37 ± 0.04	7.28 ± 0.02
MAP (mm Hg)	117 ± 12	120 ± 8	121 ± 11	110 ± 6

Readings are mean ± SD MAP, mean arterial blood pressure

Table 2. Percentages of light microscopic histological types of cortical and striatal neurons following MCA occlusion

Type[a]	Controls	Thrombosis	Clip	Clip + Nimodipine
Somatosensory cortex				
	(641)[b]	(706)	(890)	(713)
1	100	47	100	98
2	0	11	0	1
3	0	42	0	1
Striatum				
	(483)	(549)	(692)	(550)
1	100	43	99	98
2	0	19	0	1
3	0	38	1	1

[a] Histological types as follows: 1, normal (without detectable abnormalities); 2, cytoplasmic microvacuoles, clumped nuclear chromatin; 3, dark, shrunken neurons, pyknotic nuclei, and markedly dilated perineuronal spaces

[b] Total number of neurons examined in each group

No significant differences between experimental groups were demonstrated by one-way analysis of variance. Moderate hypercarbia, present in all animal groups, was probably attributable to the type of facemask used for anesthesia administration. Light and electron microscopic features of the somatosensory cortex and striatum of sham-operated control rats were unremarkable and blood vessels were free of blood.

Mechanical occlusion and recirculation

Gross inspection of all brains showed mild swelling of striatum and slightly compressed right lateral ventricles. Light microscopic analysis of thick plastic sections of striatal and cortical areas demonstrated relatively normal, well-perfused tissue (Figs. 1, 2). Mild astrocytic swelling and dilated perivascular spaces were, however, detected in some specimens. Neuronal cell counts demonstrated that less than 1% of cortical and striatal neurons appeared dark and shrunken (Table 2). In rats which underwent nimodipine treatment with clip occlusion, a similar pattern of neuronal changes was seen (Table 2).

SEM of the previously occluded MCA segment demonstrated an injured endothelial layer with few adhering platelets (Fig. 5). The damaged site was well demarcated with endothelial discontinuity being the prominent feature. A heterogeneous microvascular response to ischemia and reperfusion was detected with SEM. Some cortical and striatal vessels appeared unremarkable, while others demonstrated endothelial microvilli and dome-like structures protruding from the endothelial surface (Fig. 6).

Analysis of 1-h-perfused brain regions with TEM yielded mild to moderate neuronal, glial and microvascular changes (Figs. 9–12). Mild degrees of perivascular swelling around capillaries and arterioles were detected. Astrocytes showed mild cytoplasmic swelling and chromatin clumping (Fig. 9). Astrocytic mitochondria appeared normal and cell membranes were intact. Neuronal alterations which were most frequently seen consisted of slight chromatin clumping and dilation of endoplasmic reticulum cisternae with disaggregation of polyribosomes (Fig. 9–11). Dark shrunken neurons were seen infrequently in cortical and striatal tissues. Intraparenchymal vessels appeared well perfused, with an absence of blood cells. Endothelial cells occasionally demonstrated large cytoplasmic vacuoles which protruded into the vessel lumen, and vacuolation of tight junctional complexes (Fig. 12).

MCA thrombosis and recanalization

By gross inspection, the right hemisphere appeared pale and swollen in all rats. The right lateral ventricle was completely compressed in three of four rats. In one rat, occlusive thrombotic material was identified by gross inspection within a major lenticulostriate branch of the MCA. This rat was not used for neuronal cell counts or TEM analysis. In all other rats, microvascular beds appeared well perfused and red blood cell stasis was not observed.

Light microscopic analysis of neocortical and striatal plastic sections showed that 42% and 38% of all neurons, respectively, appeared dark and shrunken (Table 2; Figs. 3, 4). Neurons demonstrating marked chromatin clumping and cytoplasmic vacuoles were

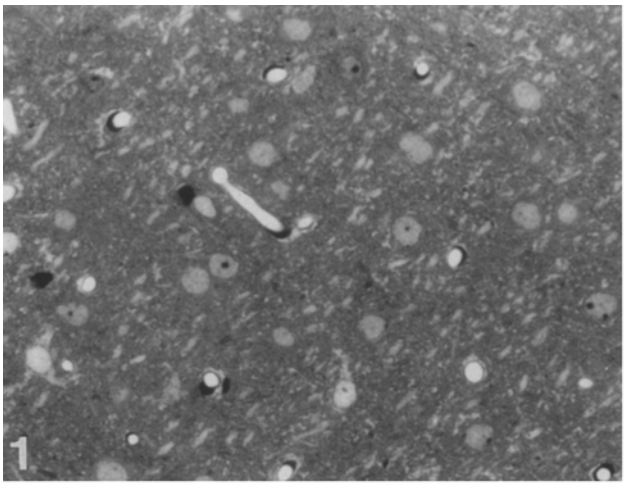

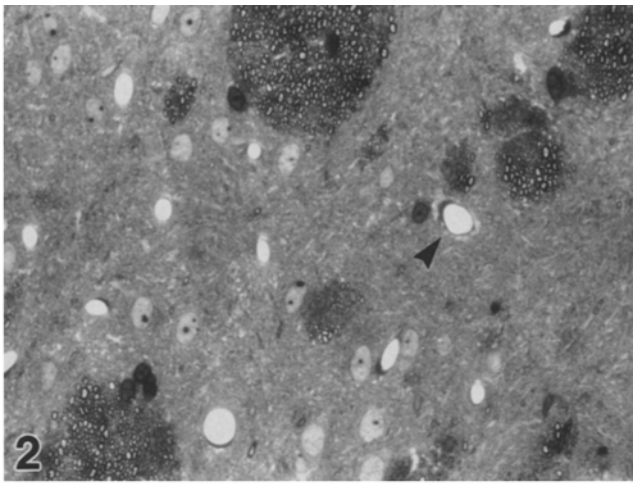

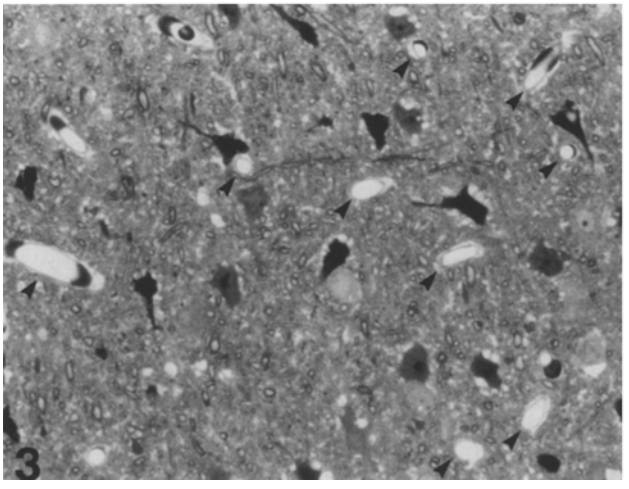

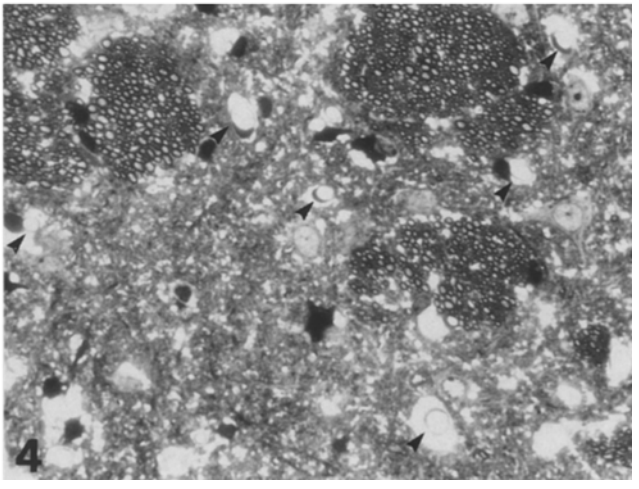

Fig. 1. Clip occlusion. Paraffin-embedded section of frontoparietal somatosensory cortex showing normal-appearing tissue. Hematoxylin-eosin, ×1100

Fig. 2. Clip occlusion. Micrograph of reperfused striatum. Mild perivascular swelling is seen (*arrowhead*). ×1100

Fig. 3. Thrombosis. Many dark shrunken neurons are shown in the somatosensory cortex 1 h following recanalization. Note that blood vessels are well perfused (*arrowheads*). ×1100

Fig. 4. Thrombosis. A vacuolated neuropil is evident in this micrograph of the striatum. Dark shrunken neurons are associated with blood vessels free of blood (*arrowheads*). ×1100

also commonly detected in these brain regions. The neuropil was vacuolated and perivascular swelling was moderate to severe in most thick sections. Although the majority of vessels displayed open lumens, moderate degrees of luminal compression were observed in some venules and capillaries. Within the somatosensory cortex, structural changes were more focal than those observed in the striatum. In some sections, columnar patterns or aggregates of dark shrunken neurons running perpendicular to the pial surface were detected. Dark neurons also appeared to be more numerous in the deeper cortical layers compared to superficial layers.

Analysis of the photochemically injured MCA segment following recanalization by SEM demonstrated thrombotic material associated with a damaged endothelial surface (Fig. 7). Although most of the luminal surface was free of thrombotic material, small and larger islets of platelet thrombi were associated with the irradiated site. Ultrastructural analysis of distal microvascular beds by SEM failed to detect luminal blood cells or platelet emboli occluding microvascular beds. Large numbers of plasmalemmal pits were, however, present on endothelial surfaces (Fig. 8).

TEM analysis of recirculated striatal and cortical areas demonstrated vacuolated neuropil (Figs. 13, 14). Swollen astrocytic processes were responsible for the vacuolated appearance. Astrocytic cell bodies were swollen and nuclei contained clumped chromatin (Fig. 15). Neuronal responses were heterogeneous, ranging from mild to severe (Figs. 13, 14). Mildly in-

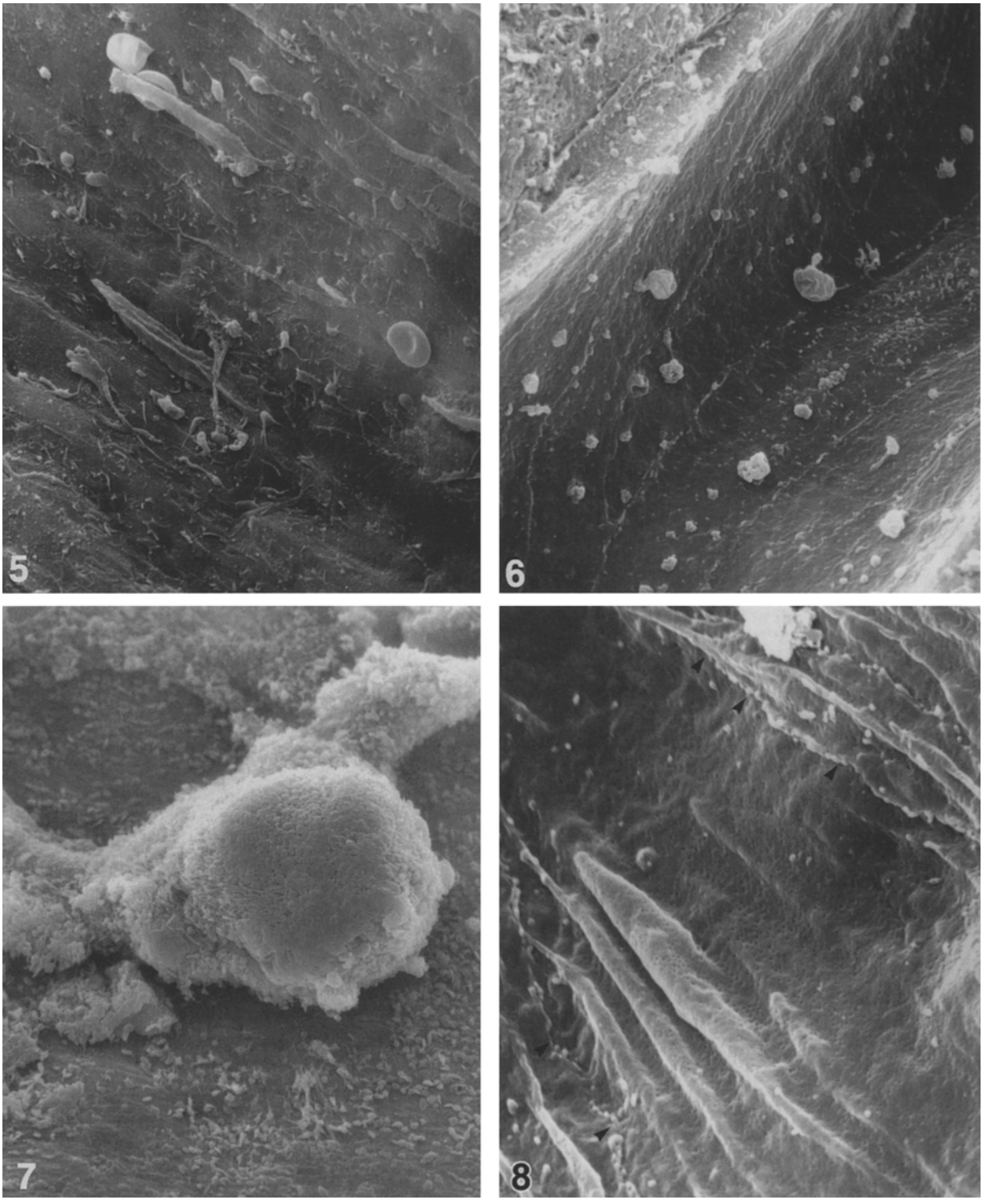

Fig. 5. Clip occlusion. Scanning electron micrograph of luminal middle cerebral artery (MCA) segment after 1 h of recirculation. Endothelial layer is damaged at clipped site. Few adhering platelets and red blood cells are present. × 1200

Fig. 6. Clip occlusion. Luminal surface of this recirculated striatal microvessel demonstrates numerous dome-like processes and microvilli protruding from the luminal surface. × 3200

Fig. 7. Thrombosis. Micrograph of irradiated MCA segment 1 h following recanalization. Note islets of platelet thrombi still present at the irradiated site. × 540

Fig. 8. Thrombosis. Striatal vessel showing large numbers of plasmalemmal pits associated with the luminal surface. Endothelial borders are indicated by *arrowheads*. × 7200

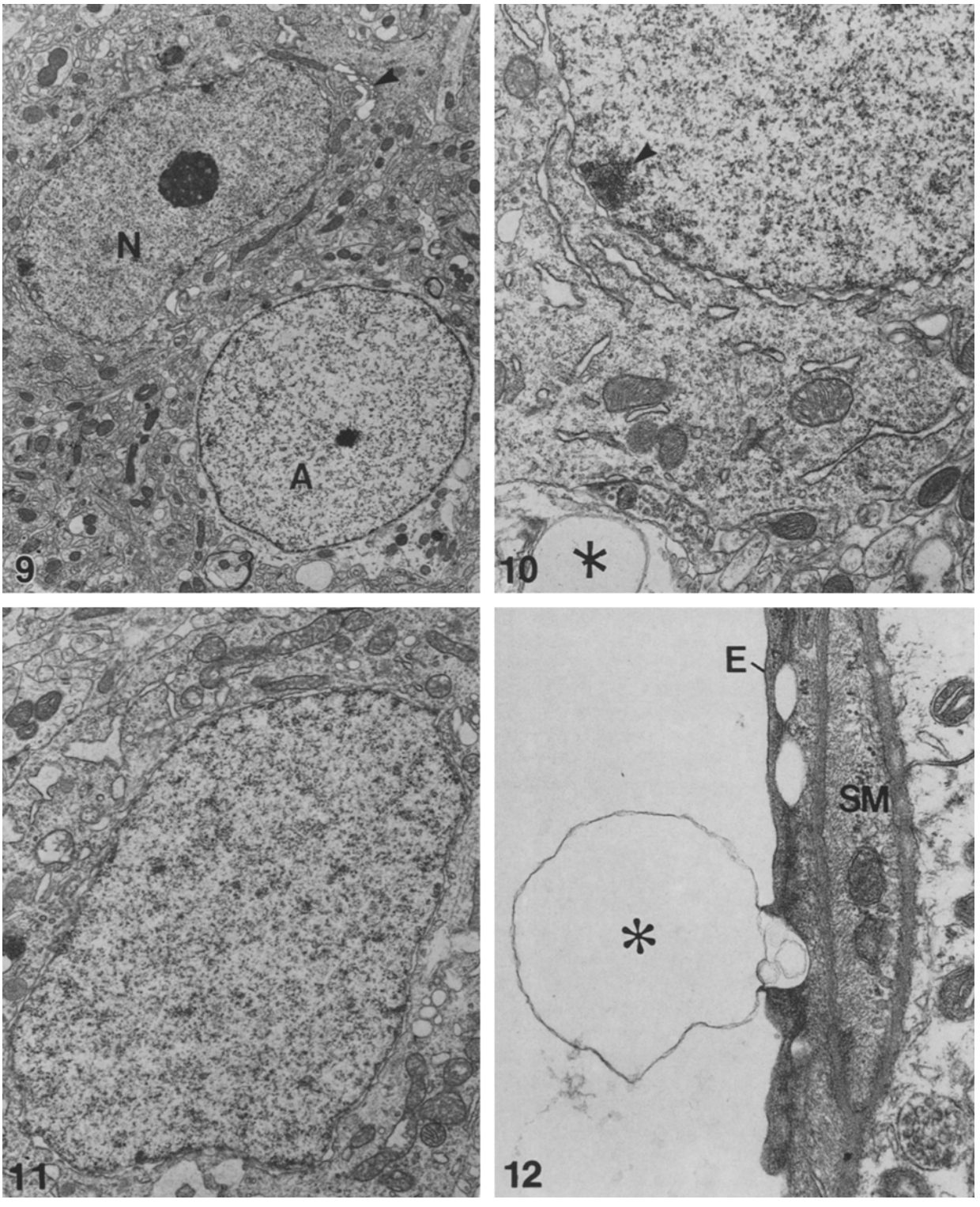

Fig. 9. Clip occlusion. Transmission electron micrograph of specimen taken from recirculated striatum. Neuron (*N*) appears unremarkable except for slight dilation of the rough endoplasmic reticulum and swelling of the Golgi apparatus (*arrowhead*). The astrocyte (*A*) is slightly swollen and neighboring neuropil appears unremarkable. ×3300

Fig. 10. Clip occlusion. This striatal neuron shows dilation of the rough endoplasmic reticulum and nuclear envelope. Chromatin is clumped (*arrowhead*). An astrocytic process (*asterisk*) is swollen. ×9700

Fig. 11. Clip occlusion. Cortical neuron demonstrating some swelling of the mitochondria and dilation of the endoplasmic reticulum. ×6300

Fig. 12. Clip occlusion. Endothelial alterations consisting of vacuolation of the endothelial tight junction and a balloon-like structure (*asterisk*) extending into the vessel lumen are seen in this reperfused cortical arteriole. *E*, Endothelium; *SM*, smooth muscle. ×25000

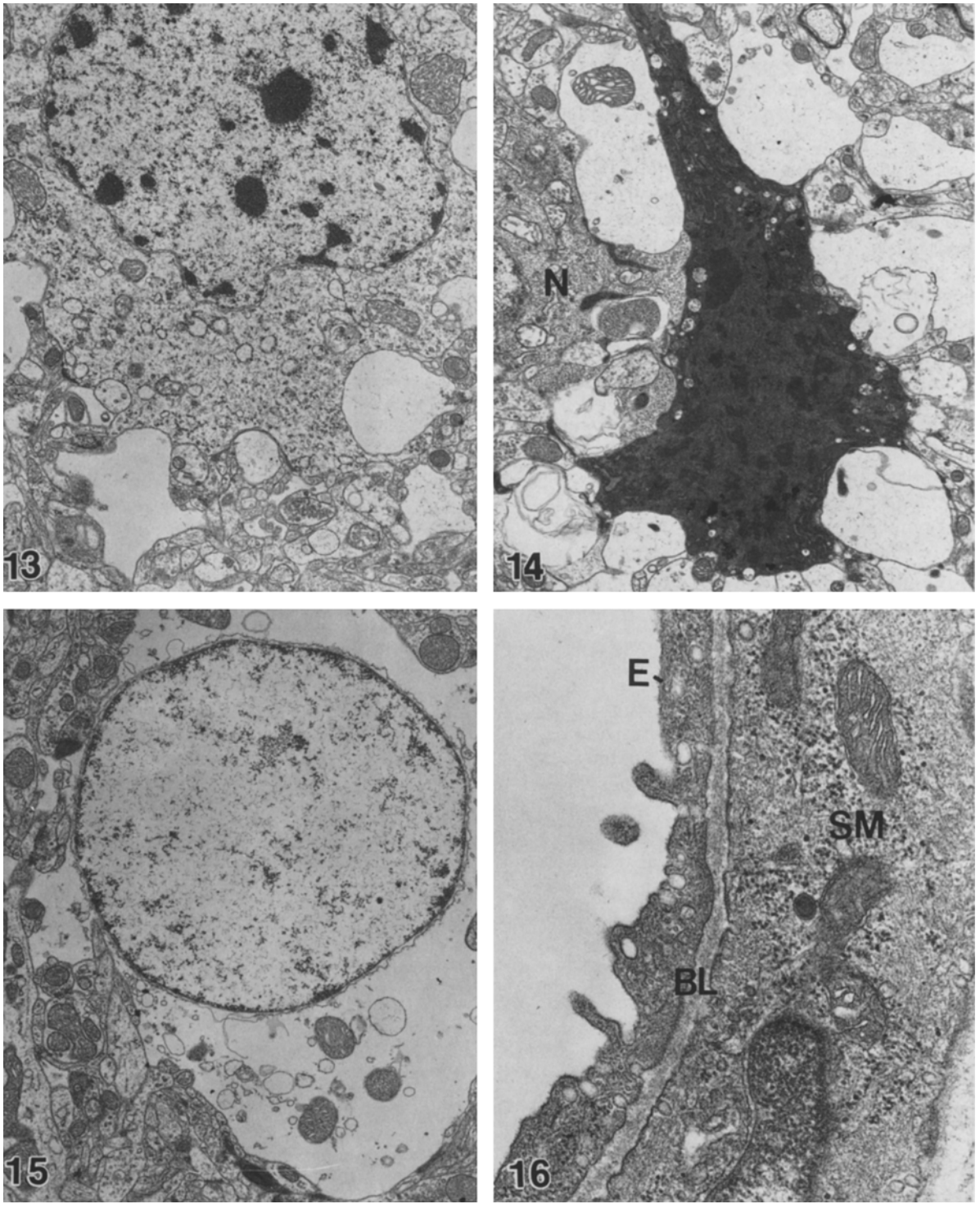

Fig. 13. Thrombosis. Striatal neuron demonstrating marked chromatin clumping and dilation of the rough endoplasmic reticulum. Perineuronal swelling is evident. × 6300

Fig. 14. Thrombosis. Cortical neuron showing type IV abnormalities, including severe shrinking of cytoplasm and nucleus, increase in electron density and dilation of mitochondria. Severe perineuronal swelling is evident. Neighboring neuron (*N*) is less severely affected but contains swollen mitochondria. × 5000

Fig. 15. Thrombosis. Swollen astrocyte within recanalized striatum is shown. × 6300

Fig. 16. Thrombosis. Pinocytotic vesicles lining luminal and abluminal membranes of an endothelial cell of a cortical arteriole. *E*, Endothelium; *BL*, basal lamina; *SM*, smooth muscle. × 19800

jured neurons manifested only slight chromatin clumping with dilation of rough endoplasmic reticulum. A second injury type consisted of neurons which displayed marked chromatin clumping and intracytoplasmic microvacuoles which corresponded to dilated endoplasmic reticulum (Fig. 13). In this group, neurons appeared slightly swollen. A third population of neurons stained with abnormal intensity and were slightly shrunken. The cytoplasm contained dilated mitochondria and endoplasmic reticulum and was surrounded by dilated astrocytic processes. Dark shrunken neurons were surrounded by severely dilated astrocytic processes (Fig. 14). Numerous microvacuoles were present throughout the condensed cytoplasm and nuclei were pyknotic and fragmented. Perivascular swelling was a consistent finding and mild degrees of vascular compression were observed. Complete compression of vessel lumina was rarely observed in this early recirculation period. Endothelial cells were occasionally vacuolated and contained large numbers of pinocytotic vesicles (Fig. 16). Tight junctions appeared intact. With TEM, thrombotic material was infrequently seen within striatal and cortical vessels.

Discussion

The results of this study indicate that experimentally induced thrombosis and recanalization of a large cerebral vessel leads to rapid and severe morphological alterations within recirculated brain regions. The severity and extent of the morphological response to vascular thrombosis, followed by recirculation, were pronounced in comparison to mechanical occlusion and recirculation. These structural differences arising between the two models do not appear to be a consequence of different ischemic severities. In rats, MCA occlusion by mechanical clips or electrocauterization produces a severe ischemic insult within the occluded MCA territory and yields predictable pathological consequences [15, 37, 41]. Thirty minutes following permanent mechanical occlusion, local cerebral blood flow (lCBF) within cerebral cortical areas is reduced to 0.24 – 0.30 ml/g per min, while in the striatum, lCBF is reduced to 0.12 ml/g per min [38]. We have recently shown that occlusive thrombosis of the MCA leads to similar reductions in lCBF [28]. Within the cortex, lCBF is reduced to 0.26 – 0.49 ml/g per min after 1 h of MCA occlusion, while in the striatum, lCBF is reduced to 0.13 ml/g per min. Severe reductions in lCBF within occluded MCA territories, therefore, occur in the two models investigated in this study.

Reperfusion of the occluded MCA segments was visually documented in both MCA models. The specially designed mechanical clip produced endothelial injury with only minor thrombotic reaction. Neuronal alterations detected after clip removal included slight chromatin clumping and dilation of the rough endoplasmic reticulum. These neuronal changes may be reversible, since unpublished data from our laboratory have demonstrated only mild histopathological striatal damage 3 days after clip removal. Microvascular alterations were also mild 1 h after clip removal and included occasional dome-like endothelial projections and endothelial microvilli. Similar endothelial lesions have been described following hypertension, concussive brain injury and cerebral ischemia [6, 7, 16, 23, 29, 43]. These endothelial alterations appear to represent nonspecific reactions to a variety of abnormal influences.

The microvascular consequences of cerebral ischemia vary depending on the duration and severity of the ischemic insult [1, 5–7, 11, 33]. In rats, 2 h of MCA occlusion results in edema formation which is resolved with recirculation [35]. In contrast, 3 h of MCA occlusion in cats results in severe brain edema and serum protein extravasation with recirculation [25]. Unpublished findings from our laboratory have demonstrated that the BBB is intact to intravenously administered horseradish peroxidase (HRP) after 1 h of MCA occlusion combined with 1 h of recirculation. Taken together, these findings illustrate the resistance of brain vessels to periods of severe incomplete ischemia [6, 11, 32].

In contrast to clip occlusion, vascular thrombosis of the MCA resulted in rapid neuronal and microvascular alterations following reperfusion. Morphological analysis of the irradiated MCA segment demonstrated that most of the occlusive thrombus was washed away following the recanalization procedure. Previous hemodynamic data obtained in this model following recanalization have demonstrated that substantial lCBF recovery occurs in most previously ischemic cortical and striatal brain regions [28]. Mean lCBF at 1 h recovers to > 50% in striatum and > 75% in cerebral cortex. In the present study, direct morphological evidence for occlusive thrombotic material in peripheral branches of the vascular territory was not consistently observed in successfully recanalized rats. It is important to emphasize that severe neuronal changes were documented in brain regions where the microcirculation appeared well perfused. Since the photochemically induced MCA thrombus is not fibrin-stabilized [8], platelet emboli from the occlusive thrombus most likely break up following recanalization, thereby decreasing the potential for intraarterial distal occlusion. Nevertheless, transient microembolization, possibly delaying postischemic lCBF normalization, is not excluded as a possible postischemic vascular event in the present study.

A high frequency of dark shrunken neurons was seen in cortical and striatal regions followings recanalization of the thrombosed artery. Similar neuronal alterations have been documented following complete ischemic insults with recirculation and with longer periods of incomplete ischemia and recirculation [4, 12, 13, 19, 20, 26]. Although the morphological correlates of irreversible ischemic neuronal injury remain controversial [19], the dense shrunken striatal neurons described in the present study represent a neuronal population that is necrotic at 7 days [28].

In the thrombotic model, the recirculated hemispheres appeared swollen and variable degrees of vascular compression were detected. Although brain water was not measured in this study, increased brain edema is consistent with the marked sponginess and parenchymal alterations described. As previously reported, experimentally induced thrombosis of the rat MCA results in acute alterations in the BBB to the protein tracer HRP [8]. The MCA occlusion models compared in this study therefore differ dramatically with respect to the acute microvascular consequences of the occlusive insult. In the thrombotic model, reperfusion into vascular beds made leaky by a combination of thrombosis and evolving ischemia, might provide excess fluid and neurotoxic substances to the injured brain tissues.

To summarize, transient occlusion of the MCA was achieved either by mechanically occluding the vessel or by thrombotic occlusion. Reperfusion of the mechanically occluded vessel resulted in subtle alterations in the previously ischemic tissue, including perivascular glial swelling and mild neuronal abnormalities. In the time frame studied, these changes are likely reversible and thus do not provide evidence of reperfusion injury. In contrast, severe neuropathological alterations in the territories of the thrombosed MCA were documented with recirculation. These parenchymal alterations are representative of reperfusion injury, inasmuch as parenchymal cells susceptible to reversible injury by ischemia per se are evidently transformed into morphological states indicative of irreversible injury. These severe alterations were probably the result of a combination of ischemic and thrombotic events. The present finding, that a rapid progression of pathological consequences is expressed during reperfusion following disintegration of an occlusive thrombus made in situ, provides impetus for the suggestion that therapeutic modalities involving thrombolysis of brain vessels must consider the problem of reperfusion injury and its mitigation [3, 27, 44].

Acknowledgements. We thank Marcila Halley for excellent technical assistance and Helen Valkowitz for typing.

References

1. Ames A, Wright RL, Kowada M, Thurston JM, Majno G (1968) Cerebral ischemia. II. The no-reflow phenomenon. Am J Pathol 52:437–453
2. Andrews BT, Lutz A, Bederson JB, Pitts LH (1986) A new microclip for vascular occlusion. J Neurosurg 64:822–823
3. Braunwald E, Kloner RA (1985) Myocardial reperfusion: a double-edged sword? J Clin Invest 76:1713–1719
4. Brown AW, Brierley JB (1972) Anoxic-ischemic cell change in rat brain: light microscopic and fine-structural observations. J Neurol Sci 16:59–84
5. Chiang J, Kowada M, Ames A, Wright RL, Majno G (1968) Cerebral ischemia. III. Vascular changes. Am J Pathol 52:455–476
6. Dietrich WD, Busto R, Ginsberg MD (1984) Cerebral endothelial microvilli: formation following global forebrain ischemia. J Neuropathol Exp Neurol 43:72–83
7. Dietrich WD, Busto R, Yoshida S, Ginsberg MD (1987) Histopathological and hemodynamic consequences of complete versus incomplete ischemia in the rat. J Cereb Blood Flow Metab 7:300–308
8. Dietrich WD, Prado R, Watson BD, Nakayama H (1988) Middle cerebral artery thrombosis: acute blood-brain barrier consequences. J Neuropathol Exp Neurol 47:443–451
9. Dietrich WD, Prado RP, Watson BD (1988) Photochemically stimulated blood-borne factors induce blood-brain barrier alterations in rats. Stroke 19:857–862
10. Fujimoto T, Walter JT Jr, Spatz M, Klatzo I (1976) Pathophysiologic aspects of ischemic edema. In: Pappius HM, Feindel W (eds) Dynamics of brain edema. Springer, Berlin Heidelberg New York, pp 171–180
11. Garcia JH, Cox JV, Hudgins, WR (1971) Ultrastructure of the microvasculature in experimental cerebral infarction. Acta Neuropathol (Berl) 18:273–285
12. Garcia JH, Kalimo H, Kamijyo Y, Trump BF (1977) Cellular events during partial cerebral ischemia. I. Electron microscopy of feline cerebral cortex after middle cerebral artery occlusion. Virchows Arch [B] 25:191–206
13. Garcia JH, Mitchem HL, Briggs L, Morawetz R, Hudetz AG, Hazelrig JB, Halsey JH, Conger KA (1983) Transient focal ischemia in subhuman primates: neuronal injury as a function of local cerebral blood flow. J Neuropathol Exp Neurol 42:44–60
14. Gotoh O, Asano T, Koide T, Takakura K (1985) Ischemic brain edema following occlusion of the middle cerebral artery in the rat. I. The time courses of the brain water, sodium and potassium contents and blood-brain barrier permeability to ^{125}I-albumin. Stroke 16:101–109
15. Gotoh O, Mohamed AA, McCulloch J, Graham DI, Harper AM, Teasdale GM (1986) Nimodipine and the haemodynamic and histopathological consequences of middle cerebral artery occlusion in the rat. J Cereb Blood Flow Metab 6:321–331
16. Hazama F, Ozaki T, Amano S (1979) Scanning electron microscopic study of endothelial cells of cerebral arteries from spontaneously hypertensive rats. Stroke 10:245–252
17. Hossmann K-A, Olssen Y (1971) The effect of transient cerebral ischemia on the vascular permeability to protein tracers. Acta Neuropathol (Berl) 18:103–112
18. Ito U, Ohno K, Nakamura R, Suganuma F, Inaba Y (1979) Brain edema during ischemia and after restoration of blood flow: measurement of water, sodium, potassium content and plasma protein permeability. Stroke 10:542–547
19. Jenkins LW, Povlishock JT, Lewelt W, Miller JD, Becker DP (1981) The role of post-ischemic recirculation in the

development of ischemic neuronal injury following complete cerebral ischemia. Acta Neuropathol (Berl) 55:205–220
20. Kalimo H, Rehncrona S, Soderfeldt B, Olsson Y, Siesjo BK (1981) Brain lactic acidosis and ischemic cell damage. 2. Histopathology. J Cereb Blood Flow Metab 1:313–327
21. Klatzo I (1967) Neuropathological aspects of brain edema. J Neuropathol Exp Neurol 26:1–14
22. Klatzo I (1987) Pathophysiological aspects of brain edema. Acta Neuropathol (Berl) 72:236–239
23. Kontos HA, Wei EP, Dietrich WD, Navari RM, Povlishock JT, Ghatak NA, Ellis EF, Patterson JL (1981) Mechanism of cerebral abnormalities after acute hypertension. Am J Physiol 240:H511–H527
24. Kuroiwa T, Ting P, Martinez H, Klatzo I (1985) The biphasic opening of the blood-brain barrier to proteins following temporary middle cerebral artery occlusion. Acta Neuropathol (Berl) 68:122–129
25. Kuroiwa T, Shibutani M, Okeda R (1988) Blood-brain barrier disruption and exacerbation of ischemic brain edema after restoration of blood flow in experimental focal cerebral ischemia. Acta Neuropathol 76:62–70
26. Little JR, Sundt TM Jr, Kerr FWL (1974) Neuronal alterations in developing cortical infarction. An experimental study in monkeys. J Neurosurg 39:186–198
27. McCord JM (1987) Oxygen-derived radicals: a link between reperfusion injury and inflammation. Fed Proc 46:2402–2406
28. Nakayama H, Dietrich WD, Watson BD, Busto R, Ginsberg MD (1988) Photothrombotic occlusion of rat middle cerebral artery: histopathological and hemodynamic sequelae of acute recanalization. J Cereb Blood Flow Metab 8:357–366
29. Nelson EG, Rennels ML, Forbes MS, Kawamura J (1975) Scanning and transmission electron microscopic studies of arterial endothelium following experimental vascular occlusion. In: Cervos-Navarro J, Betz E, Metekas F, Wuffenweber R (eds) The cerebral vessel wall. Raven Press, New York, pp 33–39
30. O'Brien MD, Jordan MM, Waltz AG (1974) Ischemic cerebral edema and the blood brain barrier. Arch Neurol 30:461–565
31. Olsson Y, Crowell RM, Klatzo I (1971) The blood-brain barrier to protein tracers in focal cerebral ischemia and infarction caused by occlusion of the middle cerebral artery. Acta Neuropathol (Berl) 18:89–102
32. Petito CK (1979) Early and late mechanisms of increased vascular permeability following experimental cerebral infarction. J Neuropathol Exp Neurol 38:222–234
33. Petito CK, Pulsinelli WA, Jacobson G, Plum F (1982) Edema and vascular permeability in cerebral ischemia: comparison between ischemic neuronal damage and infarction. J Neuropathol Exp Neurol 41:423–436
34. Schuier FJ, Hossmann K-A (1980) Experimental brain infarcts in cats. II. Ischemic brain edema. Stroke 11:593–601
35. Shigeno T, Teasdale GM, McCulloch J, Graham DI (1985) Recirculation model following MCA occlusion in rats. Cerebral blood flow, cerebrovascular permeability and brain edema. J Neurosurg 63:272–277
36. Suzuki R, Yamaguchi T, Kirino T, Orzi F, Klatzo I (1983) The effects of 5-min ischemia in Mongolian gerbils. I. Blood-brain barrier, cerebral blood flow, and local cerebral glucose utilization charges. Acta Neuropathol (Berl) 60: 207–216
37. Tamura A, Graham DI, McCulloch J, Teasdale GM (1981) Focal cerebral ischaemia in the rat. 1. Description of technique and early neuropathological consequences following middle cerebral artery occlusion. J Cereb Blood Flow Metab 1:53–60
38. Tamura A, Graham DI, McCulloch J, Teasdale GM (1981) Focal cerebral ischaemia in the rat. 2. Regional cerebral blood flow determined by [^{14}C]iodoantipyrine autoradiography following middle cerebral artery occlusion. J Cereb Blood Flow Metab 1:61–69
39. Ting P, Masaoka H, Kuroiwa T, Wagner H, Fenton I, Klatzo I (1986) Influence of blood-brain barrier opening to proteins on development of post-ischemic brain injury. Neurol Res 8:146–151
40. Tyson GW, Teasdale GM, Graham DI, McCulloch J (1982) Cerebrovascular permeability following MCA occlusion in the rat. The effect of halothane-induced hypotension. J Neurosurg 57:186–196
41. Tyson GW, Teasdale GM, Graham DI, McCulloch J (1984) Focal cerebral ischemia in the rat: topography of hemodynamic and histopathological changes. Ann Neurol 15:559–567
42. Watson BD, Dietrich WD, Prado R, Ginsberg MD (1987) Argon laser-induced arterial photothrombosis: characterization and possible application to therapy of arteriovenous malformations. J Neurosurg 66:748–754
43. Wei EP, Dietrich WD, Povlishock JT, Navari RM, Kontos HA (1980) Functional, morphological and metabolic abnormalities of the cerebral microcirculation after concussive brain injury in cats. Circ Res 46:37–47
44. Werns SW, Shea MJ, Lucchesi BR (1986) Free radicals and myocardial injury: pharmacologic implications. Circulation 74:1–5

Received September 8, 1988/Revised December 15, 1988/
Revised, accepted April 25, 1989